ESCUELA DE CONSTRUCCIÓN CIVIL
FACULTAD DE INGENIERÍA
Revista de la Construcción
Journal of Construction

Research Article

Axial compressive behavior of short tie-columns with strapping spiral ties

Milena Mesa-Lavista[1], José Álvarez-Pérez[2, *], Jorge H. Chávez-Gómez[3], G Fajardo-San-Miguel[4], Diego Cavazos-de-Lira[5], Fabián R. Ruvalcaba-Ayala[6]

1 Universidad Autónoma de Nuevo León, Facultad de Ingeniería Civil, Nuevo León (Mexico); mme-sal@uanl.edu.mx,
2 Universidad Autónoma de Nuevo León, Facultad de Ingeniería Civil, Nuevo León (Mexico); jose.alva-rezpe@uanl.mx,
3 Universidad Autónoma de Nuevo León, Facultad de Ingeniería Civil, Nuevo León (Mexico); jorge.cha-vezgm@uanl.edu.mx
4 Universidad Autónoma de Nuevo León, Facultad de Ingeniería Civil, Nuevo León (Mexico); gerardo.fajar-dosn@uanl.edu.mx
5 Universidad Autónoma de Nuevo León, Facultad de Ingeniería Civil, Nuevo León (Mexico); diego.cavazosd@uanl.edu.mx
6 Universidad Autónoma de Nuevo León, Facultad de Ingeniería Civil, Nuevo León (Mexico); fabian.ruvalca-baayl@uanl.edu.mx
*Correspondence: jose.alvarezpe@uanl.mx

Received: 17.11.2021; **Accepted:** 07.12.2022; **Published:** 29.12.2022

Citation: Mesa-Lavista, M., Álvarez-Pérez, J., Chávez-Gómez, J., Fajardo-San-Miguel, G., Cavazos-de-Lira, D. and Ruvalcaba-Ayala, F. (2022). Axial compressive behavior of short tie-columns with strapping spiral ties. Revista de la Construcción. Journal of Construction, 21(3), 657-668. https://doi.org/10.7764/RDLC.21.3.657.

Abstract: Spiral ties with rectangular cross sections have been developed as a new technology in construction, reducing the workforce in the reinforcement production series, because the worker does not have to place the tie reinforcement for the columns on the construction site. In this paper, a new type of tie was evaluated in short tie-columns subjected to axial compression to be applied in confined masonry. A comparison was made in this paper among spiral ties, with circular and rectangular cross sections, and traditional closed ties. The main aim of this research is to prove that these rectangular cross section spiral ties can be used in tie-columns for confined masonry structures. Twenty-one specimens were tested to investigate their structural behavior. As a part of the results, maximum loads, strains, load-displacement curves, and stress-strain relationships, were obtained based on testing standards, for both specimens and component materials. In addition, the fracture energy in compression and the ductility index were assessed. These results demonstrate that spiral ties with rectangular cross section have an efficient structural response compared to traditional and circular spiral ties.

Keywords: Spiral ties; strapping ties; tie-columns, experimental test, fracture energy.

1. Introduction

In the last few years, interest in the structural efficiency of confined masonry walls, used in seismic zones, has increased. Tie-columns and bond-beams are used in masonry walls to confine the masonry units and to reduce the out of plane flexural effect. This configuration adds both more ductility and more dissipation energy capacity under seismic lateral loads (Cai, Su, Tsavdaridis, & Degée, 2018). Recent investigations have focused on the influence of the ties in the structural behavior of

isolated structural elements (Du, Jin, Du, & Li, 2017; Grgić, Radnić, Matešan, & Banović, 2017; Gribniak, Rimkus, Torres, & Jakstaite, 2017; Hong, Han, & Yi, 2006; Li, Sun, Zhao, Lu, & Yang, 2018; Salah-Eldin, Mohamed, & Benmokrane, 2019; Sun & Li, 2019; Tan et al., 2018) of reinforced concrete (RC), but not in ties for tie-columns and bond beams.

The steel used to reinforce tie-columns and bond-beams in confined masonry walls differs from the steel used in RC. The rebar used in tie-columns and bond-beams is of high strength due to its cold-formed manufacture process and is of smaller diameter than the used for RC elements. The strapping forming process for the steel is usually based on thermal treatments to give more ductility to these ties.

A Mexican company (Aceros-Titán-Company, 2016) has a new technology to produce prefabricated steel cages for these structural elements, including ties with circular and rectangular cross section (Figure 1). Ties with a circular cross-section (traditional closed ties and spiral ties) are commonly used in the industry and are studied in many works (Chai & Draxler, 2014; Zhao & Wang, 2015). However, the ties with rectangular cross section are rarely used in construction. This new type of steel cage can be folded for transportation purposes making it more manageable and allowing more cages to be fitted in a tighter space, resulting in lower transportation costs.

In this paper, a new tie is studied for tie-columns and bond-beams to be applied in confined masonry. The behavior of these elements was researched from axial compressive tests in short tie-columns. A comparison was made from the load-displacement relationships by using circular and rectangular cross sections. These systems were referred to as S for strapping spiral ties (Figure 1.a), C for circular spiral ties (Figure 1.b) and, T for traditional closed ties (Figure 1.c).

The general aim is to experimentally evaluate the axial load-bearing capacity of spiral ties with rectangular cross-section against traditional closed ties, and spiral ties with circular cross-section in short tie-columns. The axial compressive phase establishes the first target for this investigation. This new tie with rectangular cross-section is cold-formed and has a thermal treatment that changes its mechanical properties (Gardner & Yun, 2018), arising the next question: will the new strapping ties satisfy the requirements for tie-column under axial compression?

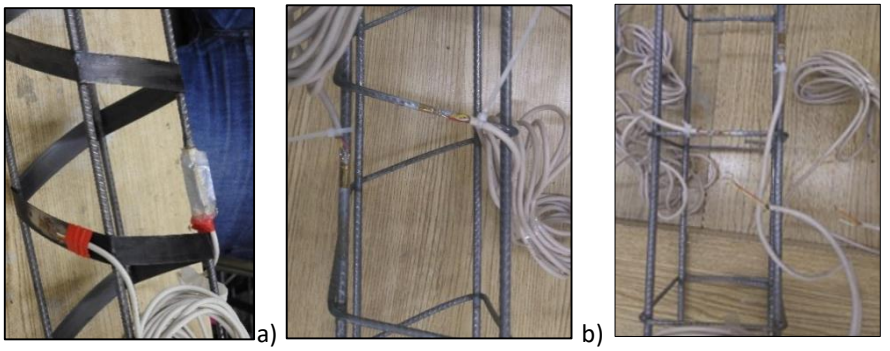

Figure 1. Ties in steel cages with: (a) Spiral with rectangular cross-section (S), (b) Spiral with circular cross-section (C) and (c) Traditional closed tie (T). (Own elaboration).

2. Materials and methods

2.1. *Material test*

In this paper three different steel were employed: (1) steel for traditional and spiral tie, with a circular cross-section; (2) steel for strapping tie, with rectangular cross-section (thermally treated steel) and, (3) steel for longitudinal rebar. The characterization of the physical mechanical properties of reinforcement steel (ASTM-A370; ASTM-E8/E8M-09) was carried out by uniaxial tensile tests (Table 1, Figure 2).

After the three types of steel were tested (ASTM-A370), a comparison of the stress-strain relationships for ties with circular cross-section and with strapping section was made. Figure 2 c, illustrates the experimental mean curves from seven specimens of both types. An increase in the elastic modulus from the strapping steel was observed. A change in its mechanical properties, due to its cold formed and thermal treatment was obtained, achieving more ductility (Table 1). The stress-strain relationship for the S steel shows a similar behavior as that proposed by X. Yun and L. Gardner (Yun & Gardner, 2017).

Table 1. Mechanical properties of steel.

Description	Longitudinal reinforcement (Ø = 6.0 mm)	Steel for T and C ties (Ø = 4.11 mm)	Steel for S ties (19 mm x 0.7 mm)
Yield stress (MPa)	527.79	332.58	489.35
Maximum stress (MPa)	656.13	583.86	652.53
Rupture stress (MPa)	472.80	399.1	597.76
Elongation at 10 Ø (%)	10.36	6	13
Elastic modulus (MPa)	145938	72426	257583
Yield Strain	0.0056	0.0066	0.0039
Strain at maximum Stress	0.16	0.073	0.13
Rupture strain	0.21	0.073	0.13
Density (kg/m^3)	7850	7850	7850

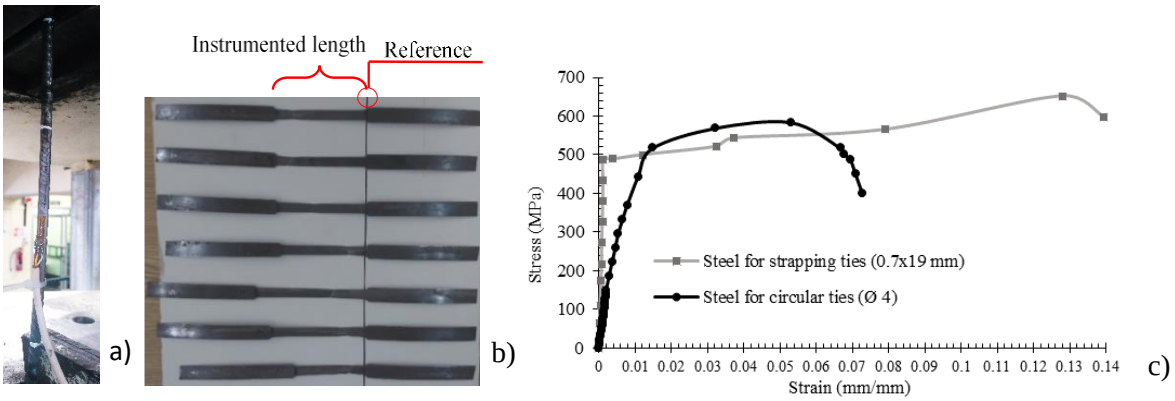

Figure 2. a) Instrumented circular tie, b) tested strapping ties, c) mean stress-strain curves of circular and strapping ties.

For the concrete, the Mexican standard (NTCM, 2017), which is renowned in many parts of Latin America (Marques & Lourenço, 2019), establish a mean compressive strength for tie-columns and tie-beams of 15 MPa, for interior and exterior walls in non-aggressive environments. In this case, the axial compressive test was carried out (Table 2, Figure 3) (ASTM-C39/C39M-18; ASTM-C617/C617M-15) in twenty-seven concrete cylinders to determine the characteristic maximum compressive strength. These cylinders were taken from a simple random sampling during the pouring of concrete and were tested at 28 days. The size of the cylinders was of 15 cm diameter and 30 cm height. The cylinders were capped as standards establish (ASTM-C39/C39M-18). The average value of the compressive strength of the concrete was 15 MPa and the coefficient of variation was $\delta = 0.0845$.

Table 2. Mechanical properties of concrete. (Own elaboration)

Compressive strength (MPa)	15
Poisson ratio	0.18
Elastic modulus (MPa)	18130
Yield strain	0.000325
Yield stress (0.4 *f'c*) (MPa)	6
Density (kg/m^3)	2000

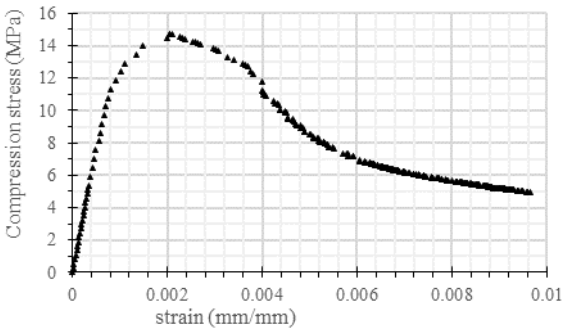

Figure 3. Mean stress-strain curves of concrete.

2.2. *Experimental test procedure*

Twenty-one specimens were tested to investigate their structural behavior and were distributed as follows: nine short tie-columns with strapping spiral ties (***S***), nine specimens with circular spiral ties (***C***) and three specimens with traditional ties (***T***). For ***S*** and ***C*** specimens, different spacings were defined (ACI-530, 2013; ASTM-A370; ASTM-C39/C39M-18; ASTM-C617/C617M-15; ASTM-E8/E8M-09; NTCM, 2017): 120 mm for the minimum, 200 mm for the maximum allowable and 158 mm for the mean. The spacing of the ***T*** specimens was of 158 mm. Table 3 summarizes the tested specimens.

The dimensions for short tie-columns were chosen to avoid lateral instability effects (JSCE, 2007): 150 mm x 150 mm x 500 mm (width x height x length). The minimum allowable longitudinal steel reinforcement was used for all the specimens (ACI-318, 2019; ACI-530, 2013), since they are used for confined masonry (ACI-318, 2019; ACI-530, 2013; JSCE, 2007). The slenderness ratio was $\frac{10}{3}$. The longitudinal reinforcement consisted of 4 Ø 6 mm for the specimens, the ***T*** and ***C*** ties were Ø 4 mm, a section of 19 mm x 0.7 mm was used for the ***S*** ties (Figure 4) All the ties had same cross-sectional area of 13.3 mm². In addition, the cover depth was of 3 cm for all the specimens (Figure 4).

Table 3. Properties for the specimens.

Ties	Tie spacing (A)	Specimens for test	Nomenclature
Strapping Spiral Tie	120 mm	3	S-12
	158 mm	3	S-15
	200 mm	3	S-20
Circular Spiral Tie	120 mm	3	C-12
	158 mm	3	C-15
	200 mm	3	C-20
Traditional Tie	158 mm	3	T-15
	Total	21	

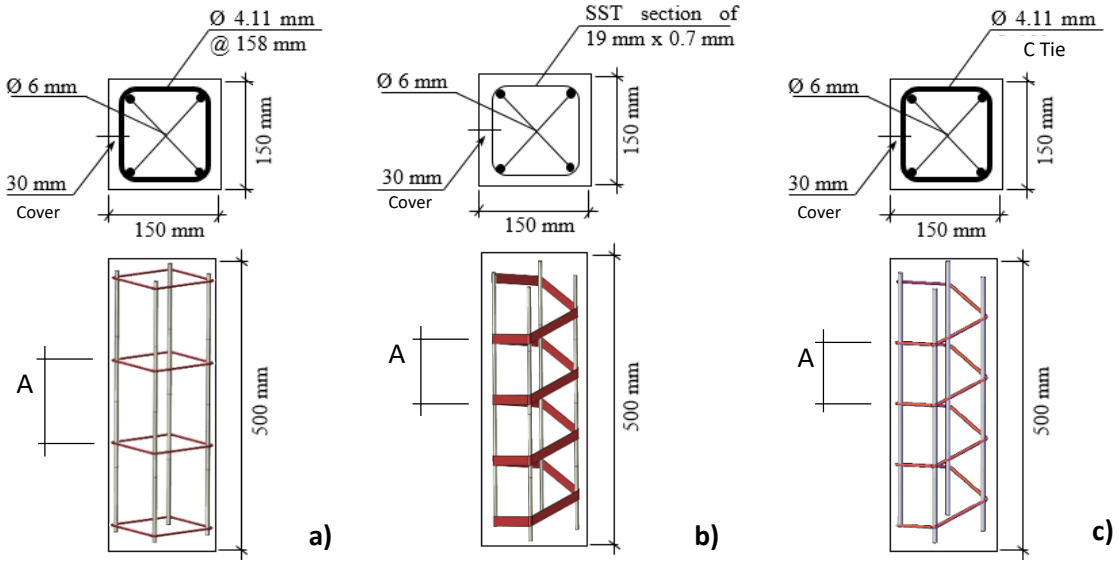

Figure 4. Geometry of the specimens: a) type T, b) type S, c) type C.

2.3. *Test setup*

The constitutive materials (steel and concrete) and the short tie-column specimens were characterized by the following measuring system: (1) Strain gauge transducers to measure strains in the concrete, (2) Strain gauge transducers to measure strains in the longitudinal steel rebar and transversal steel reinforcement and, (3) Linear variable differential transformers (LVDT) to measure the displacements of the whole specimen. A 2000 kN machine was used to test all the specimens. The post-peak behavior was determined by using a displacement-controlled test at a rate of 0.005 mm/s. Two 25 mm thick steel plates were placed at the external faces of the specimens to achieve a uniform load distribution (Figure 5). Strains were measured along the longitudinal axis of bars, ties, and the concrete surface. Figure 5 shows the schematic location of these strain transducers. These measurements were the first experimental level to determine the behavior of the new ties in the specimens.

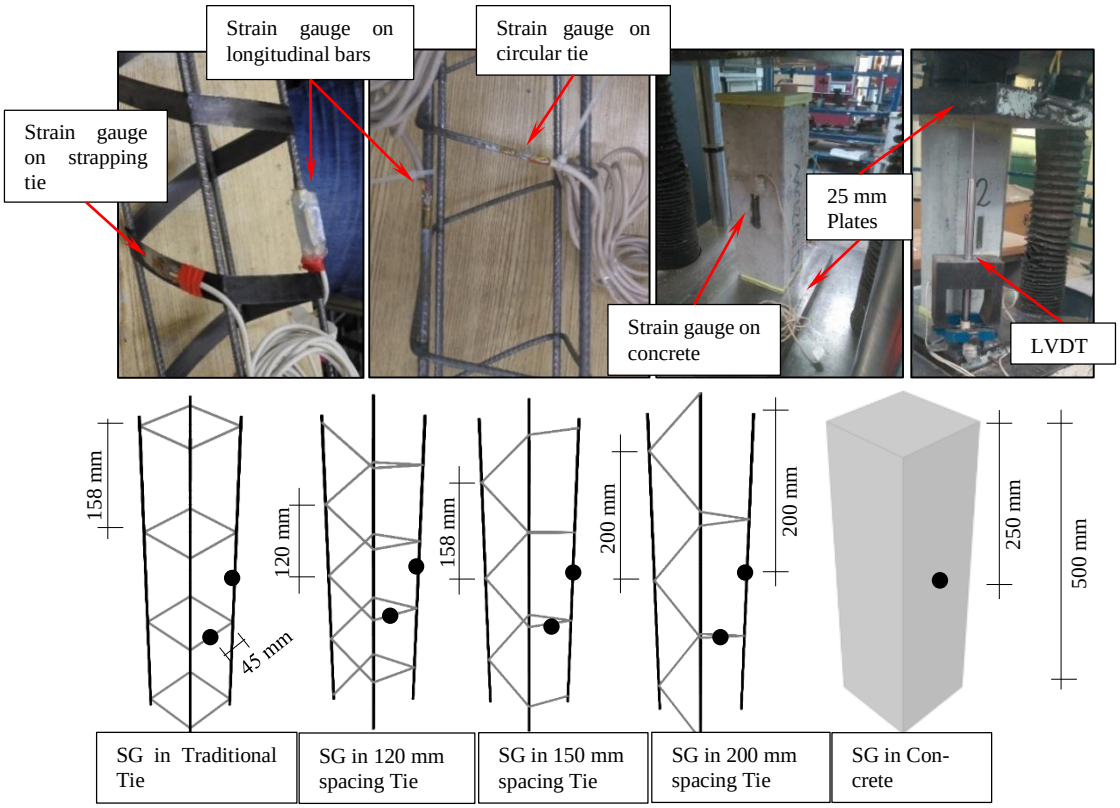

Figure 5. Instrumented specimens and schematic location of the strain gauges.

3. Results and discussions

Figure 6 a, shows the failure pattern of the sliding of the concrete in the tested specimens. This failure would be critical for isolated elements (ACI-530, 2013). This is due to the use of a minimum area of reinforcement in the tested specimens. Furthermore, Figure 6 b and c, show the loss of stability in the longitudinal bars, where a lower loss of stability was observed in ***S*** specimen.

The load-displacement curves were obtained, and are shown in Figure 7 a and b, for the tested specimens. Furthermore, the mean stiffness (E_k) evaluated at the 40% of the maximum stress from experimental relationships is shown in Figure 7 c. It can be observed that the ***S*** ties bring more stiffness to the specimens than the ***C*** ties.

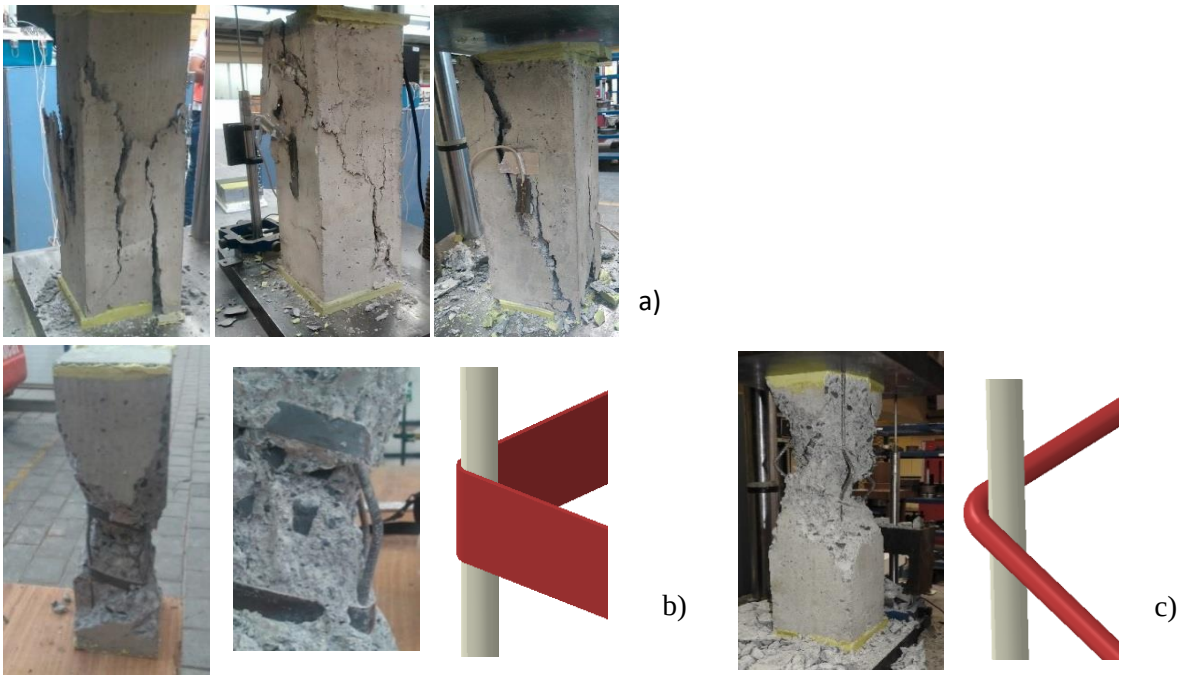

Figure 6. a) Modes of failure in the tested specimens: b) Tested specimens with strapping section, zoom in and schematic detail, c) Tested specimen with circular cross section and schematic detail.

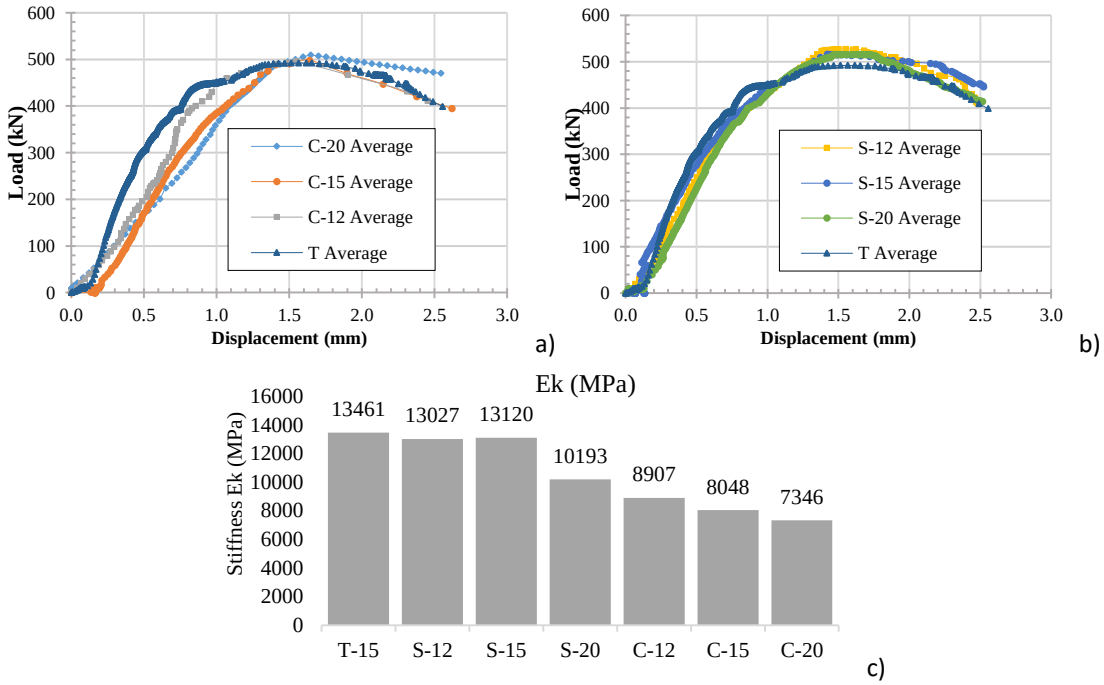

Figure 7. a) Average of the load-displacement curve for C-specimens, b) Average of the load-displacement curve for S-specimens, c) Stiffness from tested specimens.

The post-peak behavior was evaluated in each specimen in the stress-displacement relationships to obtain the fracture energy in compression (G_{fc}) (Figure 8) (Lizárraga & Pérez-Gavilán, 2017; Oller, 2001). The specimen with the S-12 tie confers 12% more ductility than the T tie specimen, as shown by Table 4.

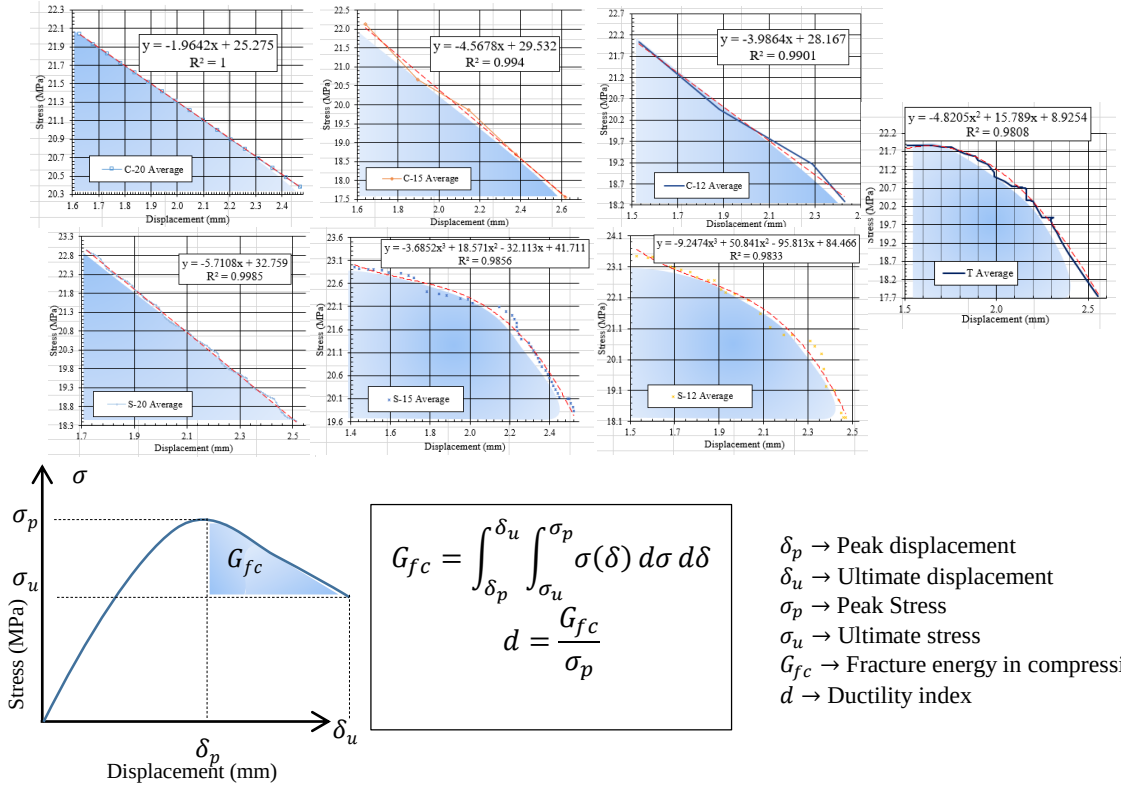

Figure 8. Curve fitting in the post-peak behavior to compute the fracture energy. Formulation to obtain the fracture energy in compression and the ductility index.

Table 4. Fracture energy in compression and ductility index (Own elaboration)

Tie	R^2	G_{fc} (N/mm)	d (mm)	Relative difference from d
T	0.9808	89.11	4.07	Control pattern
S-12	0.9833	107.00	4.56	12% (+)
S-15	0.9856	75.93	3.31	19% (-)
S-20	0.9985	74.23	3.24	20% (-)
C-12	0.9901	68.42	3.10	24% (-)
C-15	0.9940	88.77	4.01	1% (-)
C-20	1.0000	29.56	1.34	67% (-)

The mean of the maximum experimental load was also assessed from every tested system (*T*, *S*, and *C*); the relative difference was calculated by taking as a control pattern the ***T*** *tie* specimen (Figure 9). The use of ***C*** ties increased the maximum load up to 1.2%, although there was a reduction in the stiffness (Figure 7 c) and the ductility index (Table 4) when comparing against the ***T*** ties. For ***S*** ties, the maximum load increased between 5% to 7.3%. Arguably, this increment is due to a larger contact surface of ***S*** tie and the concrete (Figure 6 b). Moreover, the strapping steel had higher strength and ductility from the cold-formed process and the thermal treatment. In addition, it can be observed in Figure 6 b and c, that the longitudinal bars had better lateral confinement with the ***S*** tie than with the ***C*** tie. Due to the reduced buckling span provided by ***S*** ties, the axial load capacity of bars also improved.

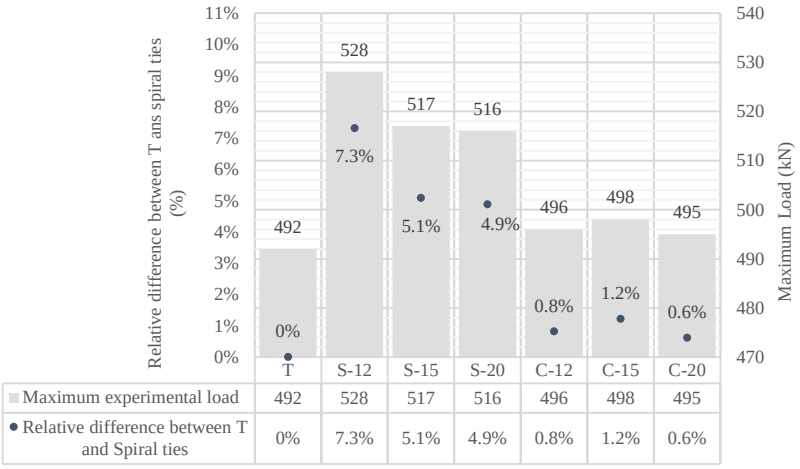

Figure 9. Average of the maximum loads from experimental results.

Furthermore, the axial design strength ($\phi P_{n,max}$) was evaluated in accordance to ACI-318 19 (Cai et al., 2018) for traditional (Eq. 1), and spiral ties (Eq. 2). When the formulas from ACI were applied, the ***T*** tie took a value of 179.5 kN (Eq. 1), and for spiral ties the value was of 220 kN (Eq. 2). Due to the ACI code does not establish any recommendations for strapping ties, the same value was used to compare the two specimens with spiral ties (*S* and *C*). Table 5 shows the relative difference between the nominal and design ACI-code strengths and the experimental results. P_n is the nominal strength of the RC.

The relative difference between both design strengths from ACI-code was 18.4% higher for spiral ties. Experimental results gave a maximum load of 528 kN for the *S-12* specimen, and 492 kN for the *T* specimen (Figure 9), with a relative difference of 7.3%. Comparing these values with those obtained from ACI-code $\phi P_{n,max}$ (ACI-318, 2019) (Eqs. 1 and 2), the experimental values were more than twice the values from ACI formulas (Table 5). The relative difference over 54% between ACI formulas and the experimental results is due to the safety factors and underestimation of the standards. The comparison with respect to the nominal strength P_n resulted in a relative difference over 28%. Equations 1 and 2, correspond to the eq. 22.4.2.1.a, and 22.4.2.1.b from the ACI-code, respectively.

$$\phi P_{n,max} = 0.8 * 0.65 * P_n \quad (1)$$

$$\phi P_{n,max} = 0.85 * 0.75 * P_n \quad (2)$$

where: $P_n = 0.85 f'c(A_g - A_{st}) + fy(A_{st})$

A_g : Gross area of the concrete section
A_{st}: Total area of the longitudinal reinforcement
f'c: Compressive strength of the concrete
fy: Yield stress of the steel

In addition, volumetric ratios of steel and concrete were obtained (Table 6). A maximum relative difference among 3% and 14% was obtained, without considering the bending of the steel in the ***T*** ties. That implies a reduction of at least 3% in the steel weight, and an increase up to a 7% in the maximum load capacity, and an improvement in the ductility index when *S-12* is used

Table 5. Relative difference between code provisions and experimental results.

Ties	Max. Load from Experiment (kN)	ACI-318 code (kN) (P_n)	Relative difference (%)	ACI-318 code (kN) ($\phi P_{n,max}$)	Relative difference (%)
T	492	345.12	29.8%	179.5	63.5%
S-12	528	345.12	34.6%	220	58.3%
S-15	517		33.2%		57.4%
S-20	516		33.1%		57.4%
C-12	486		29.0%		54.7%
C-15	489		29.4%		55.0%
C-20	485		28.8%		54.6%

Table 6. Volumetric ratios between steel and concrete.

Ties	Volume of steel (V_a) (cm^3)	Gross volume of concrete (V_c) (cm^3)	Ratio $\frac{V_a}{V_c}$ (%)	Kg of steel	Relative difference
Traditional	79.02	11250	0.70	0.62	Control pattern
S-12 and C-12	76.82		0.68	0.60	3 %
S-15 and C-15	71.75		0.64	0.56	9 %
S-20 and C-20	67.95		0.60	0.53	14 %

4. Conclusions

An experimental program was carried out in the present study to answer the question: Will the new strapping ties satisfy the requirements for short tie-columns under axial compression?

At the end of the research, the following conclusions were obtained

1. Specimens with strapping spiral tie reduce the loss of stability in the longitudinal bars due to a larger area of contact among the steel and the concrete, compared against traditional and circular spiral ties (Figure 6).
2. Short tie-columns were stiffer (Ek) with S ties than with C ties.
3. Specimen S-12 had an index of ductility 12% bigger than traditional specimens. Due to its ductility, this type of ties would be better used for confined masonry in seismic zones.
4. The strength increased from 5% up to 7.3% with the S ties with respect to the specimens with traditional ties.
5. The use of this ties decreases the needed volume of steel from 3 to 14%.
6. It is possible to use this new system of strapping spiral ties in confined masonry to increase the velocity of manufacture, while maintaining the load-capacity in axial compression unaffected.

For further investigations, longer tie-columns will be researched, including geometric nonlinearity effects and bond-beams. In addition, a micro-numerical analysis will be realized to study other zones of the element

Author contributions: Validation, Data Curation Methodology, Writing - Original Draft, Visualization. **M. Mesa-Lavista.** Conceptualization, Methodology, Formal analysis, Investigation, Writing - Original Draft, Project administration. Funding acquisition. **J. Álvarez-Pérez.** Methodology, Resources, Project administration, funding acquisition. **J. Chávez-Gómez.** Formal analysis, Writing - Review & Editing**. G. Fajardo-San Miguel.** Data Curation, Writing - Review & Editing **D. Cavazos-de-Lira**. Writing - Review & Editing. **F. Ruvalcaba –Ayala**

Funding: Project ID: PIEP-L-01-19-002-012-SC

Acknowledgments: We would like to thank Aceros Titán Company for the given information. This research would not be possible without the Structural Engineering Department support, Civil Engineering Faculty, Universidad Autónoma de Nuevo León and the PRODEP (Academic Professional Development Program).

Conflicts of interest: The authors have no conflicts of interest to declare that are relevant to the content of this article.

References

Aceros-Titán-Company. (2016). Manufacture and Distribution of steel products for the Metal-Mechanical and Construction Industries. doi:https://www.acerostitan.com/certifications

ACI-318. (2019). Building code requirements for structural concrete: (ACI 318-14); and commentary (ACI 318R-14). In. Farmington Hills, MI: American Concrete Institute.

ACI-530. (2013). Building Code Requirements and Specification for Masonry Structures and Companion Commentaries. In *TMS 602-13/4CI 530.1-13/ASCE 6-13* (pp. S-1-S-85).

ASTM-A370. Standard Test Methods and Definitions for Mechanical Testing of Steel Products. In.

ASTM-C39/C39M-18. Test Method for Compressive Strength of Cylindrical Concrete Specimens. In.

ASTM-C617/C617M-15. Standard Practice for Capping Cylindrical Concrete Specimens. In.

ASTM-E8/E8M-09. Standard test methods for tension testing of metallic materials. In A. A. State (Ed.).

Cai, G., Su, Q., Tsavdaridis, K. D., & Degée, H. (2018). Simplified Density Indexes of Walls and Tie-Columns for Confined Masonry Buildings in Seismic Zones. *Journal of Earthquake Engineering*, 1-23. doi:https://doi.org/10.1080/13632469.2018.1453396

Chai, T., & Draxler, R. R. (2014). Root mean square error (RMSE) or mean absolute error (MAE)? – Arguments against avoiding RMSE in the literature. *Geosci. Model Dev., 7*(3), 1247-1250. doi:https://doi.org/10.5194/gmd-7-1247-2014

Du, M., Jin, L., Du, X., & Li, D. (2017). Size effect tests of stocky reinforced concrete columns confined by stirrups. *Structural Concrete, 18*(3), 454-465. doi:https://doi.org/10.1002/suco.201600074

Gardner, L., & Yun, X. (2018). Description of stress-strain curves for cold-formed steels. *Construction and Building Materials, 189*, 527-538. doi:https://doi.org/10.1016/j.conbuildmat.2018.08.195

Grgić, N., Radnić, J., Matešan, D., & Banović, I. (2017). Stirrups effect on the behavior of concrete columns during an earthquake. *Materialwissenschaft und Werkstofftechnik, 48*(5), 406-419. doi:https://doi.org/10.1002/mawe.201700014

Gribniak, V., Rimkus, A., Torres, L., & Jakstaite, R. (2017). Deformation analysis of reinforced concrete ties: Representative geometry. *Structural Concrete, 18*(4), 634-647. doi:https://doi.org/10.1002/suco.201600105

Hong, K.-N., Han, S.-H., & Yi, S.-T. (2006). High-strength concrete columns confined by low-volumetric-ratio lateral ties. *Engineering Structures, 28*(9), 1346-1353. doi:https://doi.org/10.1016/j.engstruct.2006.01.010

JSCE. (2007). Standard specifications for concrete structures. In *Desing* (Vol. 15, pp. 503). Japan society of civil engineers Subcommittee on english version of standard specifications for concrete structures.

Li, W., Sun, L., Zhao, J., Lu, P., & Yang, F. (2018). Seismic performance of reinforced concrete columns confined with two layers of stirrups. *The Structural Design of Tall and Special Buildings, 27*(12), e1484. doi:https://doi.org/10.1002/tal.1484

Lizárraga, J. F., & Pérez-Gavilán, J. J. (2017). Parameter estimation for nonlinear analysis of multi-perforated concrete masonry walls. *Construction and Building Materials, 141*, 353-365. doi:https://doi.org/10.1016/j.conbuildmat.2017.03.008

Marques, R., & Lourenço, P. B. (2019). Structural behaviour and design rules of confined masonry walls: Review and proposals. *Construction and Building Materials, 217*, 137-155. doi:https://doi.org/10.1016/j.conbuildmat.2019.04.266

NTCM. (2017). Normas técnicas complementarias para el diseño y construcción de estructuras de mampostería. In (pp. 88).

Oller, S. (2001). *Mechanical fracture: a global approach (in Spanish)*. Barcelona: Centro Internacional de Métodos Numéricos en Ingeniería, .

Salah-Eldin, A., Mohamed, H. M., & Benmokrane, B. (2019). Structural performance of high-strength-concrete columns reinforced with GFRP bars and ties subjected to eccentric loads. *Engineering Structures, 185*, 286-300. doi:https://doi.org/10.1016/j.engstruct.2019.01.143

Sun, L., & Li, W. (2019). Cyclic behavior of reinforced concrete columns confined with two layers of stirrups. *Structural Concrete, 0*(0). doi:https://doi.org/10.1002/suco.201800229

Tan, R., Eileraas, K., Opkvitne, O., Žirgulis, G., Hendriks, M. A. N., Geiker, M., . . . Kanstad, T. (2018). Experimental and theoretical investigation of crack width calculation methods for RC ties. *Structural Concrete, 19*(5), 1436-1447. doi:https://doi.org/10.1002/suco.201700237

Yun, X., & Gardner, L. (2017). Stress-strain curves for hot-rolled steels. *Journal of Constructional Steel Research, 133*, 36-46. doi:https://doi.org/10.1016/j.jcsr.2017.01.024

Zhao, Y., & Wang, F. (2015). Experimental studies on behavior of fully grouted reinforced-concrete masonry shear walls. *Earthquake Engineering and Engineering Vibration, 14*(4), 743-757. doi:10.1007/s11803-015-0030-5